Electronic Supplementary Material (ESI) for *Sustainable Energy & Fuels*.
This journal is © The Royal Society of Chemistry 2019

Fabrication of NH_2-MIL-125 Nanocrystals for High Performance Photocatalytic Oxidation

Xiuniang Tan,[a, b] Jianling Zhang,*[a, b, c] Jinbiao Shi,[a, b] Xiuyan Cheng,[a, b] Dongxing Tan,[a, b] Bingxing Zhang,[a, b] Lifei Liu,[a, b] Fanyu Zhang,[a, b] Buxing Han [a, b, c] and Lirong Zheng [d]

[a] Beijing National Laboratory for Molecular Sciences, CAS Key Laboratory of Colloid, Interface and Chemical Thermodynamics, CAS Research/Education Center for Excellence in Molecular Sciences, Institute of Chemistry, Chinese Academy of Sciences, Beijing 100190, P.R.China.

[b] School of Chemical Sciences, University of Chinese Academy of Sciences, Beijing 100049, P.R.China..

[c] Physical Science Laboratory, Huairou National Comprehensive Science Center, Beijing 101400, P.R.China.

[d] Beijing Synchrotron Radiation Facility (BSRF), Institute of High Energy Physics, Chinese Academy of Sciences, Beijing 100049, P.R.China.

*E-mail: zhangjl@iccas.ac.cn.

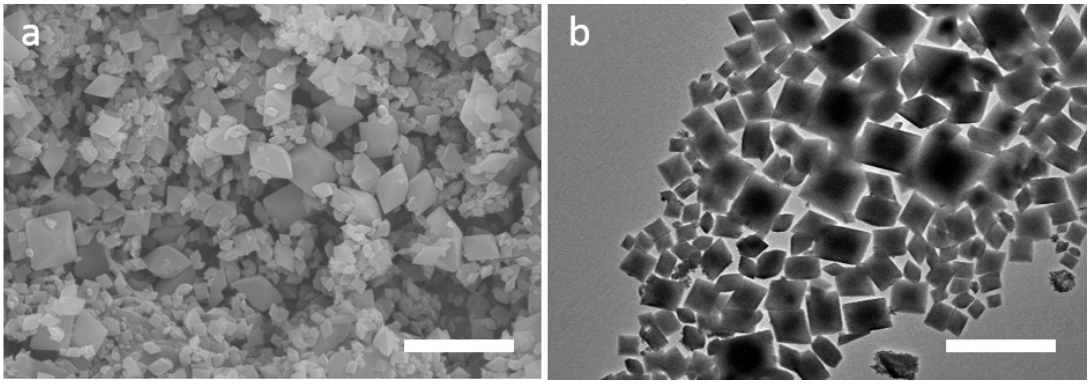

Fig. S1 SEM image (a) and TEM image (b) of *m*-NH_2-MIL-125. Scale bars, 5 µm in (a) and 2 µm in (b).

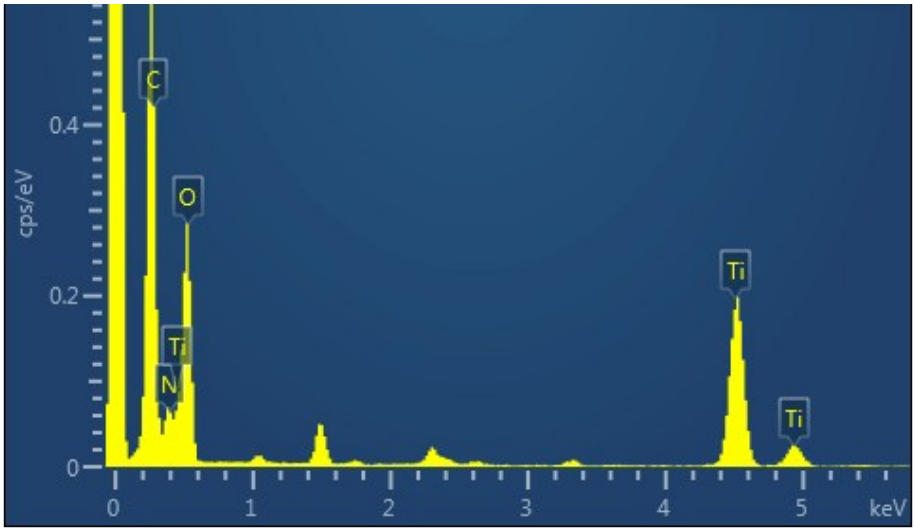

Fig. S2 EDX spectrum of *n*-NH_2-MIL-125.

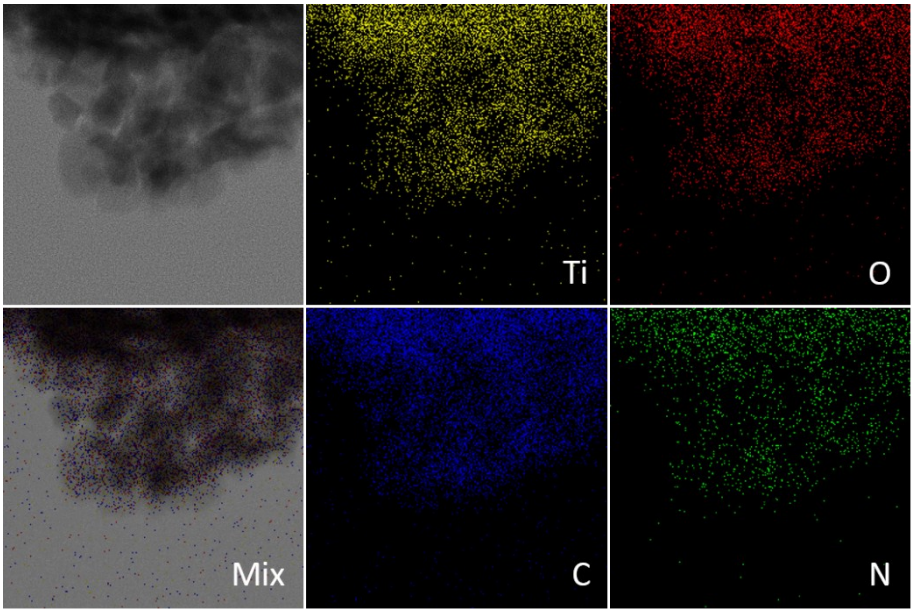

Fig. S3 EDX elemental mapping of *n*-NH_2-MIL-125.

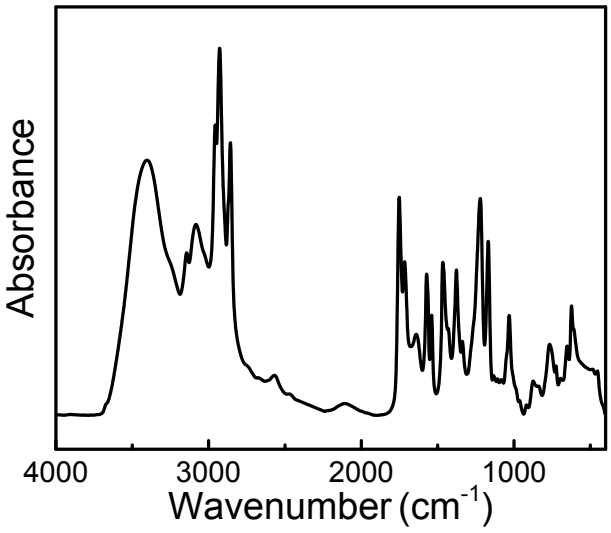

Fig. S4 FT-IR spectrum of OmimAc. The characteristic absorptions of OmimAc are C-H vibrations of imidazolium ring at 3144 and 3082 cm^{-1}, absorption bands of acetate at 1751 and 1716 cm^{-1}, and skeleton stretching vibrations of imidazolium ring at 1466 and 1169 cm^{-1}.

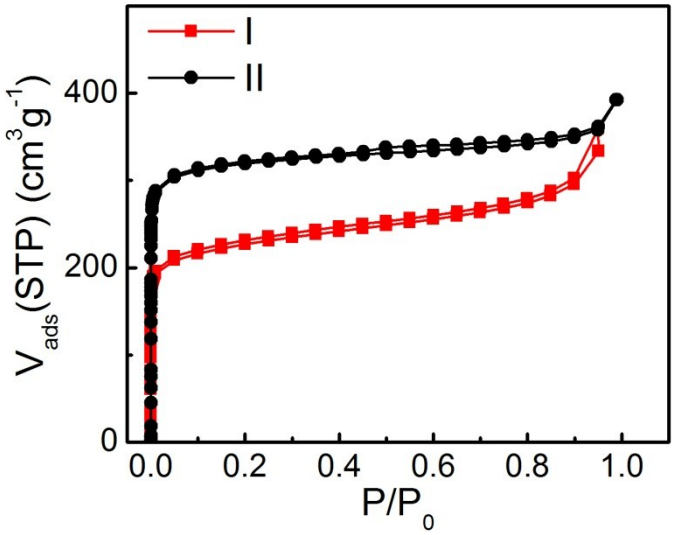

Fig. S5 N_2 adsorption-desorption isotherms of *n*-NH_2-MIL-125 (I) and *m*-NH_2-MIL-125 (II).

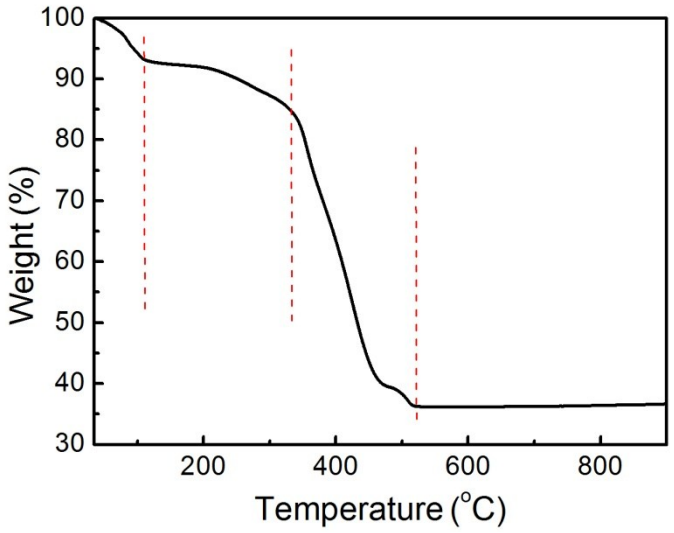

Fig. S6 TG curve of *n*-NH_2-MIL-125. It displays three steps for mass losses. From 35 to 100 °C, the weight loss corresponds to the removal of guest molecules methanol. The mass loss between 100 and 330 °C corresponds to the desorption of the non-coordinated ligand NH_2-H_2BDC trapped in *n*-NH_2-MIL-125. The main weight loss in the region of 330 to 520 °C results from the decomposition of the framework to produce TiO_2. The thermal stability of *n*-NH_2-MIL-125 is similar with the reported NH_2-MIL-125.[1,2]

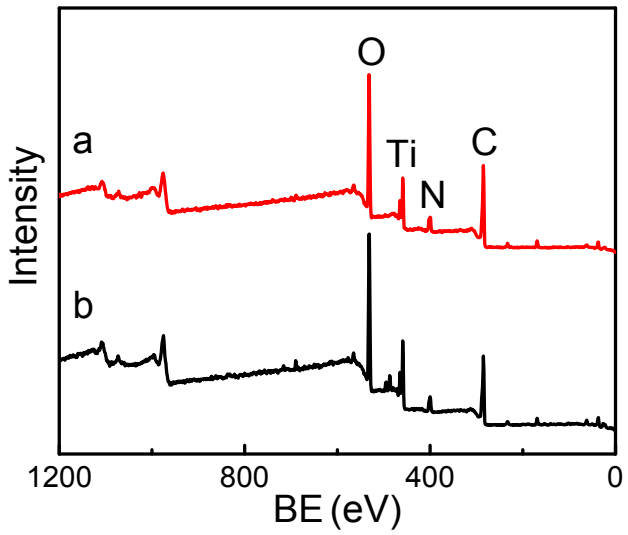

Fig. S7 Survey XPS spectra of the *n*-NH_2-MIL-125 (a) and *m*-NH_2-MIL-125 (b).

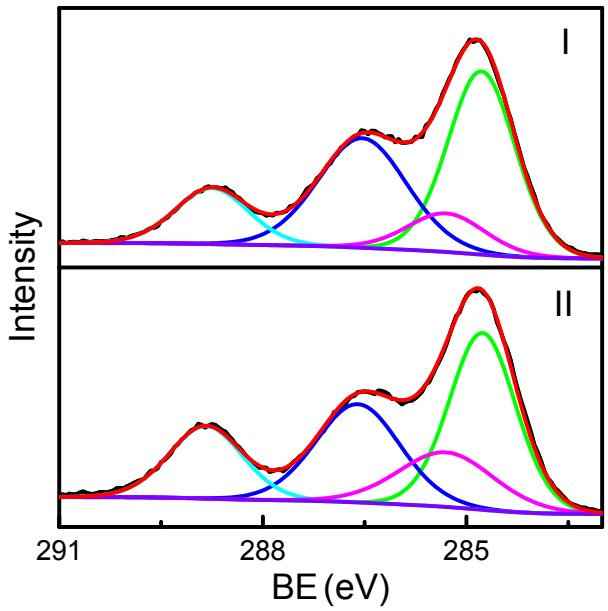

Fig. S8 C 1s XPS spectra of *n*-NH_2-MIL-125 (I) and *m*-NH_2-MIL-125 (II). The four carbon bonds C=C, C-N, C-C and C=O located at 284.8, 285.3, 286.5 and 288.8 eV, respectively, coincide with the molecular structure of the MOF.

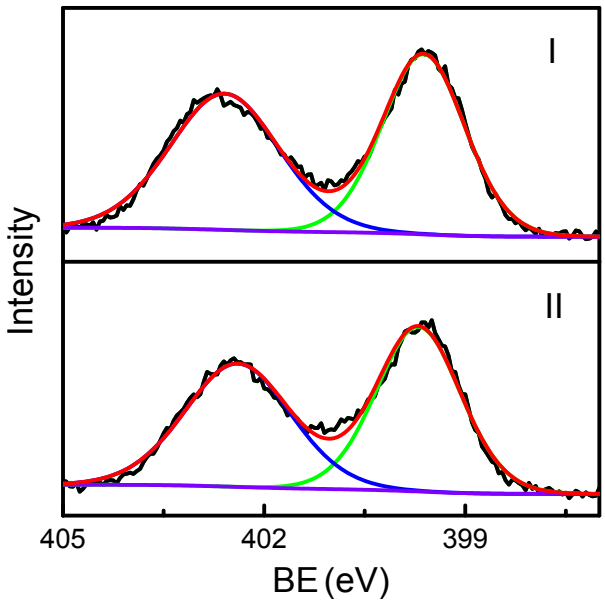

Fig. S9 N 1s XPS spectra of *n*-NH_2-MIL-125 (I) and *m*-NH_2-MIL-125 (II). The two bands are assigned to the N of -NH_2 protruding into or stretching out the cavities (399.6 eV) and the positively charged N (-NH-$^+$ or -N=$^+$, 402.6 eV), respectively.

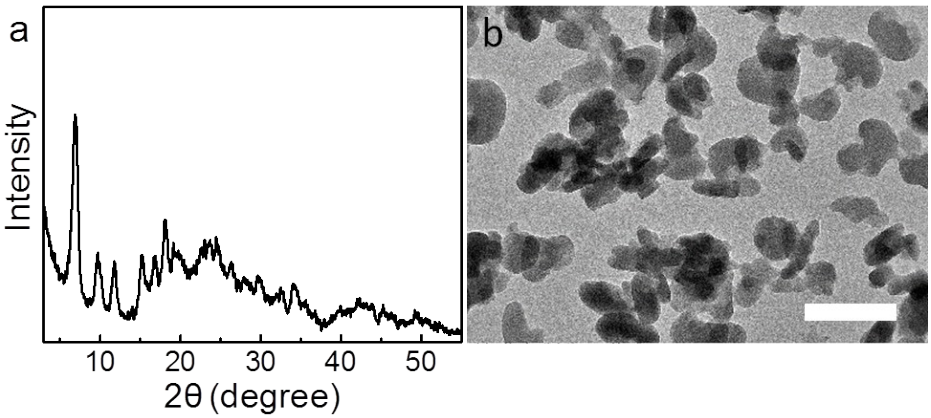

Fig. S10 XRD pattern (a) and TEM image (b) of the reused *n*-NH_2-MIL-125. Scare bar, 200 nm.

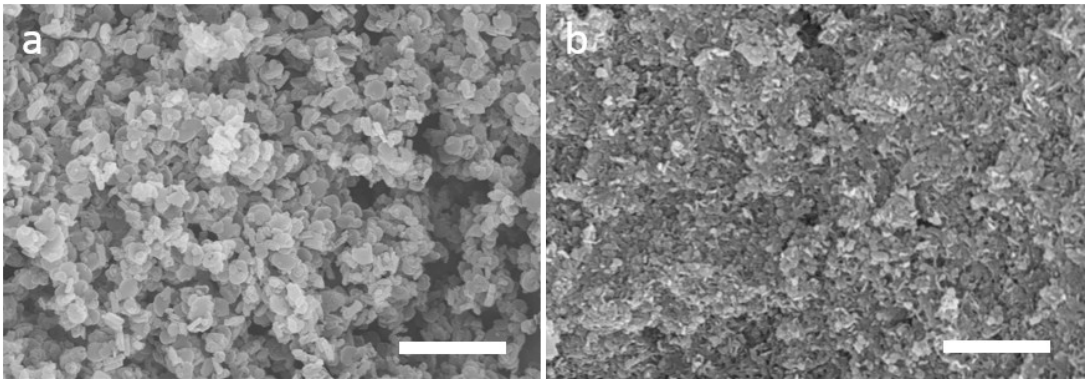

Fig. S11 SEM images of NH_2-MIL-125 nanocrystals synthesized by using different amounts of OmimAc: 0.1 g mL^{-1} (a) and 0.3 g mL^{-1} (b) for OmimAc to DMF/MeOH. Scale bars, 2.5 µm in (a) and 1 µm in (b).

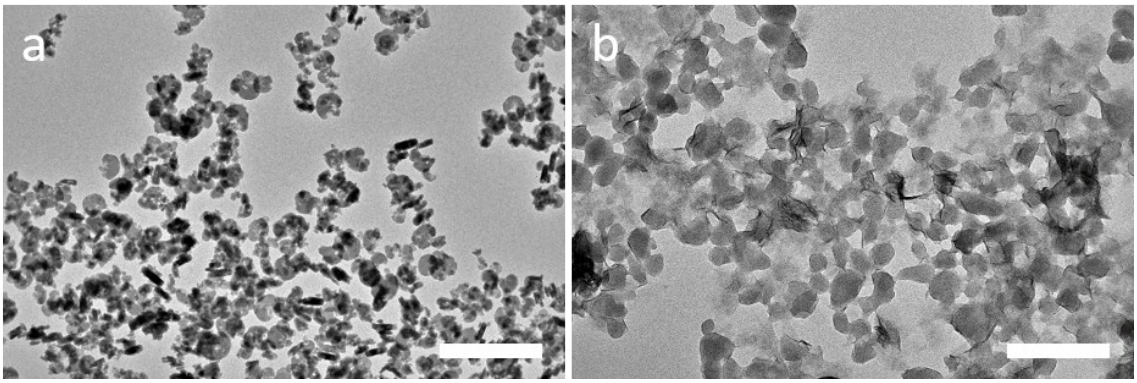

Fig. S12 TEM images of NH_2-MIL-125 nanocrystals synthesized by using different amounts of OmimAc: 0.1 g mL^{-1} (a) and 0.3 g mL^{-1} (b) for OmimAc to DMF/MeOH. Scale bars, 2 µm in (a) and 200 nm in (b).

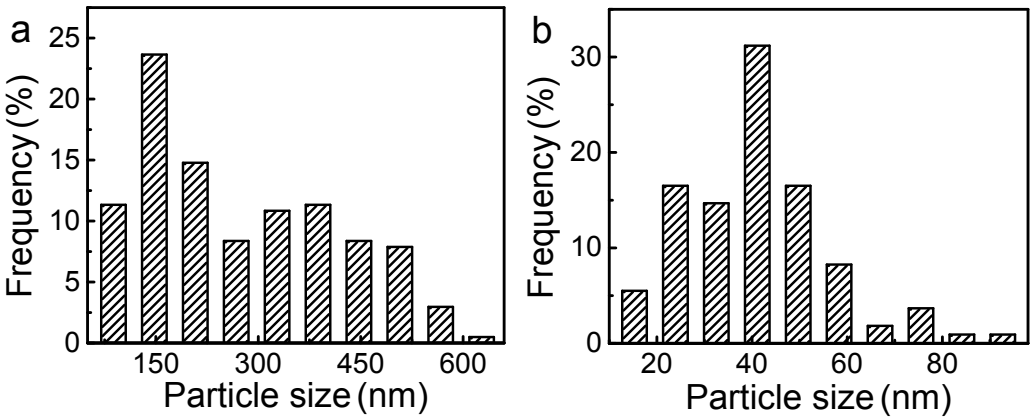

Fig. S13 Size distributions of NH_2-MIL-125 particles synthesized by using different amounts of OmimAc: 0.1 g mL^{-1} (a) and 0.3 g mL^{-1} (b) for OmimAc to DMF/MeOH.

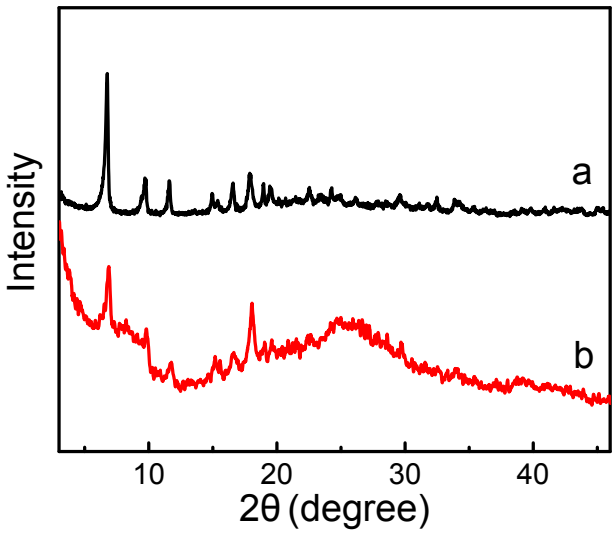

Fig. S14 XRD patterns of NH_2-MIL-125 nanocrystals synthesized by using different amounts of OmimAc: 0.1 g mL^{-1} (a) and 0.3 g mL^{-1} (b) for OmimAc to DMF/MeOH.

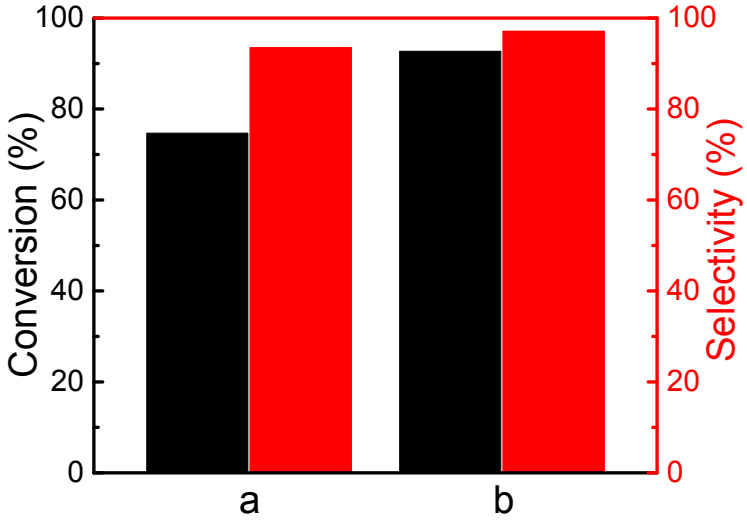

Fig. S15 Photocatalytic performances of NH_2-MIL-125 nanocrystals synthesized by using different amounts of OmimAc for benzylamine into N-benzylbenzaldimine at 9 h: 0.1 g mL^{-1} (a) and 0.3 g mL^{-1} (b) for OmimAc to DMF/MeOH.

Table S1 Comparison of different photocatalysts for benzylamine oxidation into N-benzylbenzaldimine.

Photocatalyst	Reaction condition	Conversion (%)	Selectivity (%)	TOF (μmol g^{-1} h^{-1})	Reference
n-NH_2-MIL-125	0.2 mmol amine, 10 mg catalyst, 4 mL MeCN, 300 W Xe lamp (350-780 nm), air, 25 ^oC, 9 h	98.5	99.0	1063	This work
m-NH_2-MIL-125	0.2 mmol amine, 10 mg catalyst, 4 mL MeCN, 300 W Xe lamp (350-780 nm), air, 25 ^oC, 9 h	55.9	93.5	570	This work
NH_2-UiO-66	0.1 mmol amine, 15 mg catalyst, 3 mL MeCN, 350 W Xe lamp (full range), air, RT, 10 h	83	99	277	3
TiO_2	0.1 mmol amine, 10 mg catalyst, 5 mL MeCN, air, 100 W Hg lamp (>300 nm), 9 h	99	85	472	4
	500 W Xe lamp (>350 nm), 5 h	93	87	809	
Nb_2O_5	5 mmol amine, 100 mg catalyst, 10 mL benzene, 500 W Hg lamp (>300 nm), O_2, RT, 50 h	>99	97	485	5
Ag/AgI/Titanate	0.5 mmol amine, 50 mg catalyst, 10 mL MeCN, 500 W Hg lamp, O_2, 40 ^oC, 24 h	95	96	190	6
(Zn^{II}/Ti^{IV})LDH	0.2 mmol amine, 20 mg catalyst, 5 mL MeCN, 500 W Hg lamp (>300 nm), air, 5 h	100	97	970	7
NH_2-MIL-125	0.1 mmol amine, 5 mg catalyst, 2.0 mL MeCN, 300 W Xe lamp (420-800 nm), O_2, 12 h	73	86	523	8

References

1 Y. H. Fu, D. R. Sun, Y. J. Chen, R. K. Huang, Z. X. Ding, X. Z. Fu and Z. H. Li, *Angew. Chem. Int. Ed*., 2012*,* **51***,* 3364-3367.
2 Z. H. Rada, H. R. Abid, J. Shang, Y. D. He, P. Webley, S. M. Liu, H. Q. Sun and S. B. Wang, *Fuel*, 2015, **160**, 318-327.
3 R. X. Liu, S. Y. Meng, Y. L. Ma, L. T. Niu, S. H. He, X. Q. Xu, B. T. Su, D. D. Lu, Z. W. Yang and Z. Q. Lei, *Catal. Commun*., 2019, **124**, 108-112.
4 X. N. Lang, H. W. Ji, C. C. Chen, W. H. Ma and J. C. Zhao, *Angew. Chem. Int. Ed*., 2011, **50**, 3934-3937.
5 S. Furukawa, Y. Ohno, T. Shishido, K. Teramura and T. Tanaka, *ACS Catal*., 2011, **1**, 1150-1153.
6 Z. F. Zheng, C. Chen, A. Bo, F. S. Zavahir, E. R. Waclawik, J. Zhao, D. J. Yang and H. Y. Zhu, *ChemCatChem*, 2014, **6**, 1210-1214.
7 X.-J. Yang, B. Chen, X.-B. Li, L.-Q. Zheng, L.-Z. Wu and C.-H. Tung, *Chem. Commun.*, 2014, **50**, 6664-6667.
8 D. R. Sun, L. Ye and Z. H. Li, *Appl. Catal. B: Environ.*, 2015, **164**, 428-432.